Long-range Response to Local Grid Modifications in AC Electricity Grids

D. Jung[1] S. Kettemann[1]

[1] Department of Physics & Earth Sciences, Focus Area Health, Jacobs University Bremen, Campus Ring 1, 28759 Bremen, Germany

d.jung@jacobs-university.de s.kettemann@jacobs-university.de

SPONSORED BY THE Federal Ministry of Education and Research

Abstract

Local changes in the topology of electricity grids can cause overloads far away from the disturbance [1], making the prediction of the robustness against power outages a challenging task. The impact of single-line additions on the long-range response of DC electricity grids has recently been studied [2]. By solving the steady state AC load flow equations, we extend the investigation to the case of alternating currents. Later, we are going to use these steady state results in order to study the time-dependent spreading of local phase perturbations throughout the grid, following a new approach from a recent analytical study [3].

Power flow in an AC grid

Complex power flow equations

→ From *Ohm's law* and *Kirchhoff equations*, deduce the *steady state power flow equations* (PFE) for a 1-phasic AC network,

$$S_i - V_i \sum_j Y_{ij}^* (V_i - V_j)^* = 0 \quad . \qquad (1)$$

Here, $S_i = P_i + iQ_i$ is the *net generated power* entering the electricity grid at node i, with P_i the *active power* and Q_i the *reactive power*, and $i,j \in \{1,2,\ldots,N\}$, with N the number of nodes.

Complex PFEs for an inductive grid

→ Assume a purely *inductive* grid and sinusoidal voltages. *Admittance* of edge (i,j) (representing a transmission line):

$$Y_{ij} = \frac{1}{i\omega L_{ij}} \quad , \qquad (2)$$

⇒ By doing so, we can assume constant voltage magnitudes, $|V_i| \equiv V_0$ [3].

→ Define *power capacity* of edge (i,j) [3]:

$$K_{ij} = \frac{V_0^2}{\omega L_{ij}} \quad . \qquad (3)$$

→ Consider voltage *phase angles* $\varphi_i(\omega,t) = \omega t + \theta_i(t)$, with the *grid frequency* $\omega = 2\pi \cdot 50\,\mathrm{Hz}$ [3].

→ Thereby, the *PFEs* (1) can be rewritten as

$$S_i = i \sum_j K_{ij} \left(1 - e^{i(\theta_i - \theta_j)}\right) \quad . \qquad (4)$$

Real part of the power flow equations

→ In this study, we only consider the real part of the PFEs:

$$P_i = \sum_j K_{ij} \sin(\theta_i - \theta_j) \quad . \qquad (5)$$

⇒ Disregard *reactive power*.

⇒ System of N nonlinear equations, solvable by a standard *root-finding algorithm*[1] in order to find the *phase distribution* θ_i.

→ Afterwards, compute the *transmitted power*

$$F_{ij} = K_{ij} \sin(\theta_i - \theta_j) \qquad (6)$$

for each edge (i,j) of the graph.

Model

→ Cyclic square 2D grid graph, size $N = l^2$.

→ Binary distribution for nodal *net generated power* $P_i \in \{-P_0, +P_0\}$. Condition $\sum_i P_i = 0$ must be fulfilled, so the linear system size l must be an even number.

→ Consider constant *power capacities* $K_{ij} = K_0$.

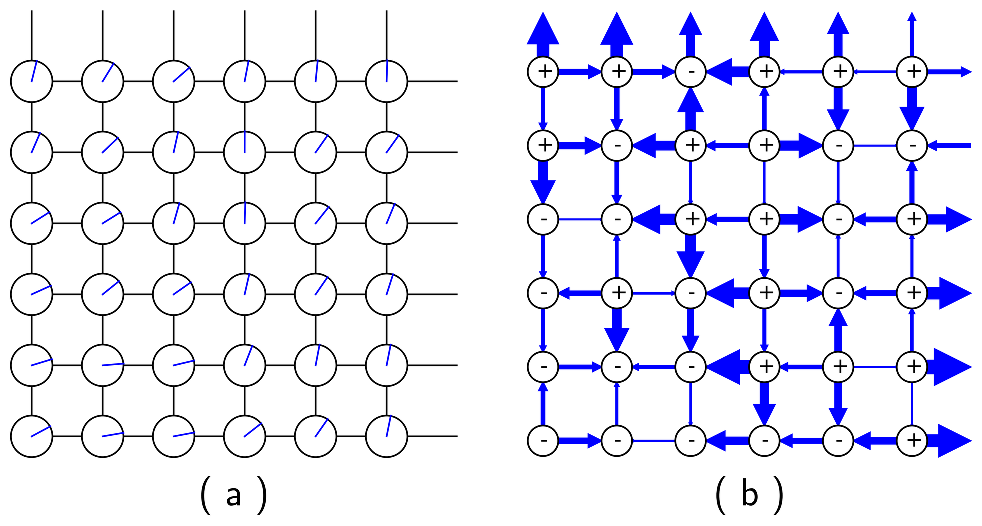

Figure 1: *(a) Phase distribution θ_i of a 6×6 system with binary distribution of the nodal net generated power $P_i \in \{-P_0, +P_0\}$. (b) Resulting power flow. The size of the arrow is proportional to the transmitted power F_{ij}.*

Response to adding another transmission line

→ Add another "diagonal" transmission line somewhere in the grid and observe the change of power flow $\Delta F_{ij} = F_{ij}^{\text{after}} - F_{ij}^{\text{before}}$ for each transmission line (i,j).

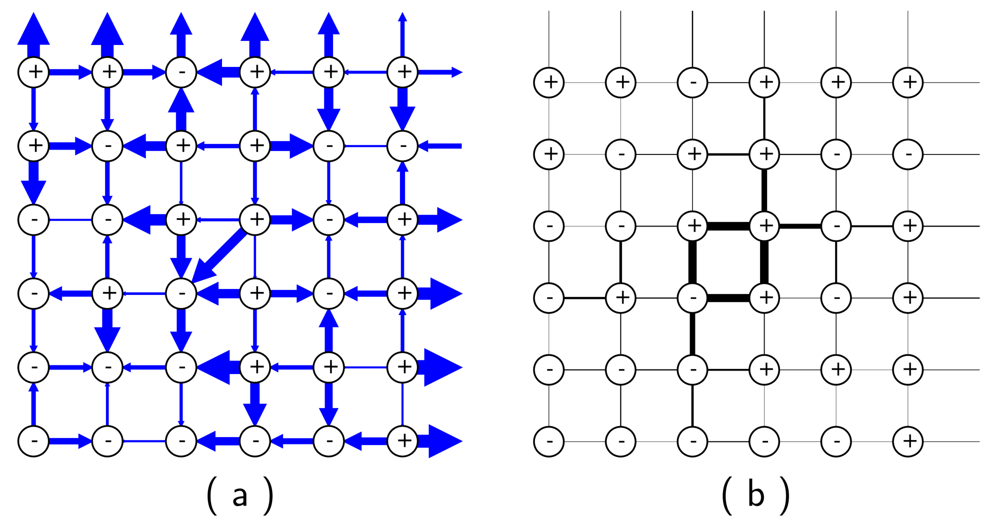

Figure 2: *(a) Power flow of the same system as in Fig. 1 after the addition of another transmission line. (b) Change of transmitted power after adding the line. The width of each line is proportional to the absolute change of transmitted power, $|\Delta F_{ij}|$.*

→ To analyze response properties, define the distance r_{ij} of the edge (i,j) to the added edge (see Fig. 3).

→ Average $|\Delta F_{ij}|$ over all edges (i,j) with the same distance r to the disturbance, and over $R = 1000$ realizations of disorder.

→ Realizations for which no stable solution can be found are skipped.

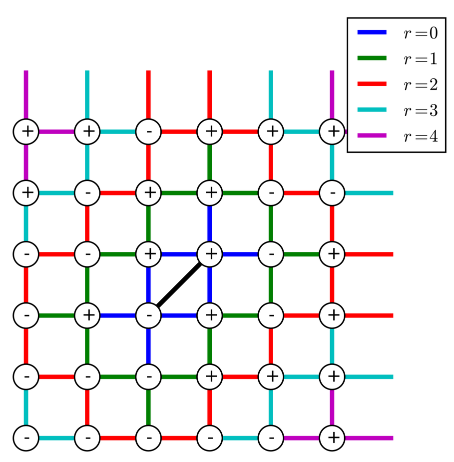

Figure 3: *Classification of the transmission lines by their distance r to the added line (black).*

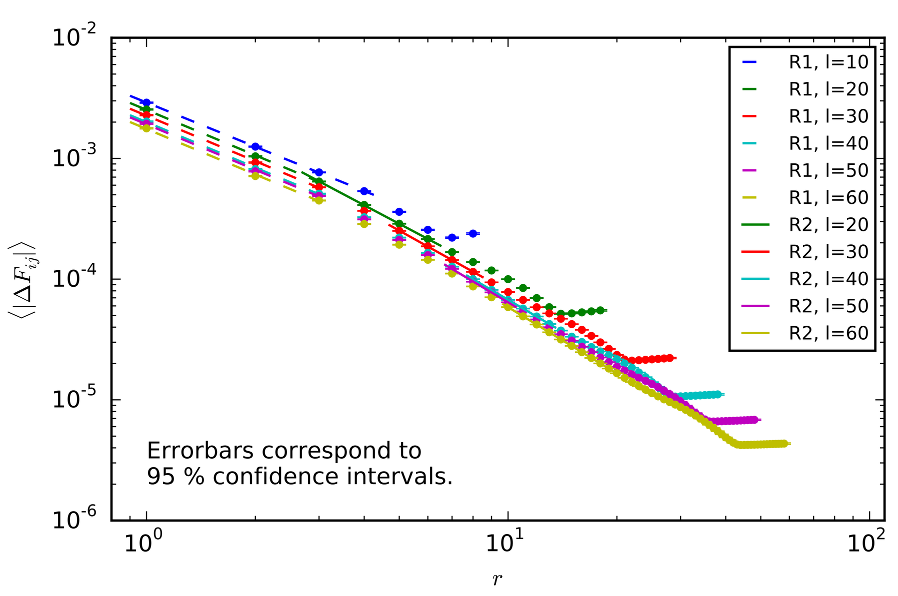

Figure 4: *Double-logarithmic plot of $\langle|\Delta F_{ij}|\rangle(r)$ for different system sizes l. For the regimes R1 ($r \le 3$) and R2 ($r \ge 3$), the data has been fitted to a power law (7).*

→ We observe a *power law* behavior of $\langle|\Delta F_{ij}|\rangle(r)$ (see Fig. 4). We fit the data to the fit model

$$f(r) = ar^{-b} \quad . \qquad (7)$$

→ Two regimes R1 and R2 can be distinguished, roughly separated by $r = 3$, with different exponents b_{R1} and b_{R2}. Tab. 1 and 2 summarize the fit results for both regimes.

→ $\langle|\Delta F_{ij}|\rangle$ saturates for $r \to L$ (or even slightly increases again). The saturation values themselves (for which $r = l-2$) decay as a power law with increasing system size l (see Fig. 5(b)).

Table 1: *Fit results for regime R1 (short range behavior). For each system size l, only data for $r_{\min} \le r \le r_{\max}$ is considered. To assess the quality of the fit, χ^2 and the quality of fit probability Q are given.*

l	$r_{\min}$	$r_{\max}$	N_D	a	b	χ^2	Q
10	1	4	4	0.00291 ± 0.00002	1.217 ± 0.005	2.46	0.29
20	1	3	3	0.00252 ± 0.00006	1.250 ± 0.026	17.88	0.00
30	1	3	3	0.00226 ± 0.00007	1.252 ± 0.035	29.38	0.00
40	1	3	3	0.00200 ± 0.00006	1.253 ± 0.038	33.85	0.00
50	1	3	3	0.00192 ± 0.00006	1.253 ± 0.039	37.32	0.00
60	1	3	3	0.00175 ± 0.00006	1.253 ± 0.040	38.27	0.00

Table 2: *Fit results for regime R2 (long range behavior).*

l	$r_{\min}$	$r_{\max}$	N_D	a	b	χ^2	Q
20	3	6	4	0.00369 ± 0.00005	1.586 ± 0.009	3.22	0.52
30	5	8	4	0.00371 ± 0.00009	1.671 ± 0.012	3.50	0.48
40	8	13	6	0.00388 ± 0.00005	1.760 ± 0.006	3.12	0.54
50	7	10	4	0.00390 ± 0.00011	1.783 ± 0.014	3.19	0.53
60	10	19	10	0.00393 ± 0.00002	1.826 ± 0.002	3.27	0.51

Finite-size scaling

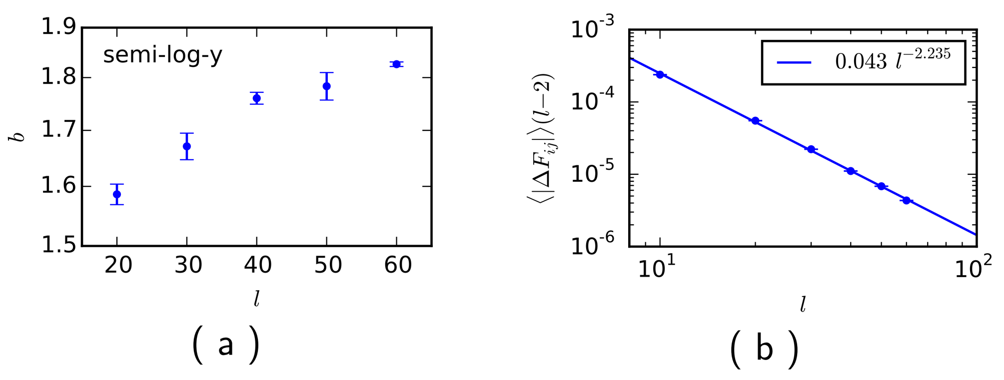

Figure 5: *(a) Dependence of the exponent b on the linear system size l (regime R2). (b) Scaling behavior of saturation value $\langle|\Delta F_{ij}|\rangle(r = l-2)$ on system size l.*

Long-range response in DC electricity grids

→ It is worthwhile to compare these results to a recent study on the long-range response in DC electricity grids [2].

→ Considering constant link conductances $Y_{ij} \in \mathbb{R}$, *ohmic resistances* as well as Joule's heating $\mathrm{d}P_{ij}^{\Omega}$ [2].

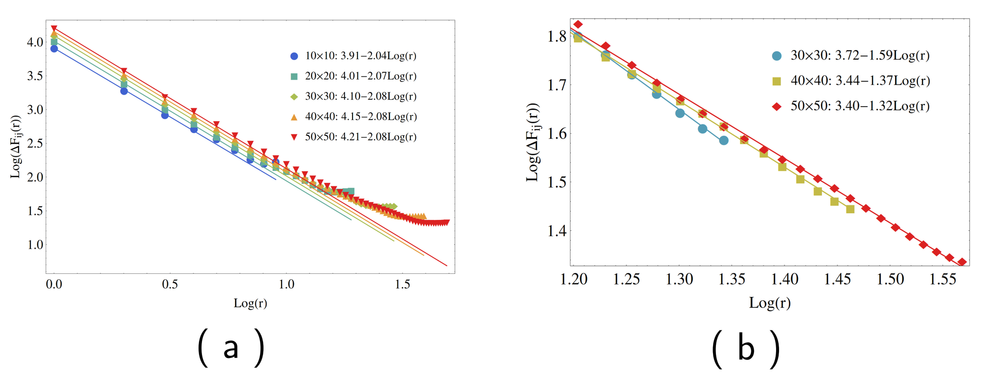

Figure 6: *Change of DC power flow ΔF_{ij} in dependence of the distance r to the added link [2]. (a) Regime R1, (b) regime R2.*

→ Finding power law dependence as well, but with different exponents $b_{\mathrm{DC,R1}}$ and $b_{\mathrm{DC,R2}}$ (see Fig. 6).

→ In DC system, $b_{\mathrm{DC,R1}} > b_{\mathrm{DC,R2}}$, whereas in AC system, $b_{\mathrm{R1}} < b_{\mathrm{R2}}$.

→ $b_{\mathrm{DC,R2}}$ decreases with increasing system size l, thus showing an opposing behavior to AC results [2].

→ Saturation value (not shown here) also scales as a power law with system size, but with a rather different exponent $d_{\mathrm{DC}} \approx 1.36$ [2].

Conclusions

→ We have found a short as well as a long range response to local grid modifications.

→ The data of the long range regime fits nicely to a power law, whereas the short range regime leads to poor fits.

→ Results are similar to those of DC grids, but exponents and finite-size scaling behavior are quite different, e.g. $b_{\mathrm{R2}} = 1.826 \pm 0.002$ vs. $b_{\mathrm{DC,R2}} = 1.32$ (each for the largest considered system size).

Outlook

→ Application to other topologies including *real-world topologies*.

→ Study time-dependent spreading of local phase perturbations, following a recently published approach [3]. Clarify the role of *Anderson localization* in AC transmission grids.

Acknowledgements

→ The numerical calculations have been performed using computational resources of the Computational Laboratories for Analysis, Modeling and Visualization (CLAMV), Jacobs University Bremen, Germany.

→ We greatfully acknowledge support of BMBF, CoNDyNet, FK. 03SF0472A.

References

[1] D Witthaut, M Timme. *The European Physical Journal B* **86**, 377 (2013).

[2] D Labavić, R Suciu, H Meyer-Ortmanns, S Kettemann. *European Physical Journal Special Topics* **223**, 2517 (2014).

[3] S Kettemann. *Phys. Rev. Lett., under review, arxiv:1504.05525* (2015).

[4] E Jones, T Oliphant, P Peterson, Others. SciPy: Open source scientific tools for Python (2007).

[5] J. J Moré, B. S Garbow, K. E Hillstrom. User guide for MINPACK-1. Technical Report ANL-80-74, Argonne National Laboratory, Argonne, IL, USA (1980).

[1]We use the Python function `scipy.optimize.fsolve` [4], which is a wrapper around the functions `hybrd` and `hybrj` of the Fortran package `MINPACK` [5].

CoNDyNet STROMNETZE Forschungsinitiative der Bundesregierung